

# Enabling Efficient Dynamic Resizing of Large DRAM Caches via A Hardware Consistent Hashing Mechanism

Kevin K. Chang<sup>†</sup>, Gabriel H. Loh<sup>\*</sup>, Mithuna Thottethodi<sup>‡</sup>, Yasuko Eckert<sup>\*</sup>, Mike O'Connor<sup>\*</sup>, Srilatha Manne<sup>\*</sup>, Lisa Hsu<sup>\*</sup>, Lavanya Subramanian<sup>†</sup>, and Onur Mutlu<sup>†</sup>

<sup>†</sup>Carnegie Mellon University   <sup>\*</sup>AMD Research   <sup>‡</sup>Purdue University

## Abstract

*Die-stacked DRAM has been proposed for use as a large, high-bandwidth, last-level cache with hundreds or thousands of megabytes of capacity. Not all workloads (or phases) can productively utilize this much cache space, however. Unfortunately, the unused (or under-used) cache continues to consume power due to leakage in the peripheral circuitry and periodic DRAM refresh. Dynamically adjusting the available DRAM cache capacity could largely eliminate this energy overhead. However, the current proposed DRAM cache organization introduces new challenges for dynamic cache resizing. The organization differs from a conventional SRAM cache organization because it places entire cache sets and their tags within a single bank to reduce on-chip area and power overhead. Hence, resizing a DRAM cache requires remapping sets from the powered-down banks to active banks.*

*In this paper, we propose CRUNCH (Cache Resizing Using Native Consistent Hashing), a hardware data remapping scheme inspired by consistent hashing, an algorithm originally proposed to uniformly and dynamically distribute Internet traffic across a changing population of web servers. CRUNCH provides a load-balanced remapping of data from the powered-down banks alone to the active banks, without requiring sets from all banks to be remapped, unlike naive schemes to achieve load balancing. CRUNCH remaps only sets from the powered-down banks, so it achieves this load balancing with low bank power-up/down transition latencies. CRUNCH's combination of good load balancing and low transition latencies provides a substrate to enable efficient DRAM cache resizing.*

## 1. Introduction

Die-stacking technologies are rapidly maturing [21, 31]. One likely near-term use is to stack a processor with a large, high-bandwidth, in-package DRAM cache [4, 18, 23]. Projections indicate that the size of the DRAM cache may be hundreds of megabytes or more. Many workloads (or workload phases) may not productively utilize such large caches, however. This leads to wasted energy consumption because of significant DRAM background power (from leakage and peripheral circuitry). Recent studies have shown that a system's DRAM is consuming an increasing fraction of the overall system power [14, 25]. While a die-stacked DRAM's overall capacity will be less than that of main memory (and therefore not likely to consume nearly as much power as off-chip DRAM),

in the present age of power-constrained designs, any power consumed by the stacked DRAM is power that cannot be consumed by the CPU cores [10].

Thus, there is opportunity to reduce the energy consumption of the die-stacked DRAM cache while maintaining the performance advantages of having a large-capacity caching structure. When the DRAM cache is under-utilized, it should reduce its active portions to match the capacity needs of the current workload. This can be achieved by turning off some banks of the DRAM cache. While turning off ways/banks is a well-studied problem in the context of SRAM caches [2, 30, 32, 40], the organization of the DRAM cache poses new challenges. Current proposals for DRAM cache organizations [7, 23, 26] call for entire sets and their tags to reside within a single bank in order to reduce the number of row activations per access. Hence, a DRAM cache resizing mechanism would need to (1) consider not only which banks to turn off (well-explored problem in SRAM caches) but also (2) address the new challenge of remapping sets from the powered-down banks into active banks (or suffer 100% miss rates for those addresses) and migrating the dirty data from the powered-down banks to either the active banks or to the off-chip DRAM.

Naive data remapping when resizing a DRAM cache can be very costly. One possible way to do this is to remap all of the data from a powered-down bank into another active bank. This remapping scheme could make the active bank a hotspot, increasing DRAM cache access latencies. Another possibility is to completely remap data from all banks to the remaining active banks with a modulo- $k$  operation ( $k$ =number of active banks after a bank shut-down), providing a uniform distribution of data among the active banks without creating hotspots. However, completely remapping data across all banks every time the cache size changes can be very costly, as this requires migrating a large amount of dirty data.

To address the challenge of remapping data in a load-balanced manner with low transition overhead, we take inspiration from the *consistent hashing* algorithm originally proposed to uniformly and dynamically distribute load across a large number of web servers [19]. Cloud providers may have servers go down at any point in time (e.g., server crashes, scheduled maintenance). Similarly, new servers may come online (e.g., machines rebooted, adding new machines to the server pool). The frequency of machines coming and going

make it infeasible to perform a complete re-indexing each time the pool of available servers changes.

Consistent hashing provides an elegant scheme where a machine failure results in re-indexing *only the subset of elements that mapped to that machine*. That subset is redistributed among the surviving machines in a load-balanced manner; at the same time, any elements already mapped to the remaining machines remain where they are. Turning off DRAM cache banks is analogous to servers going down (and turning on banks is like servers coming online). In this work, we present a hardware remapping scheme inspired by consistent hashing, called *Cache Resizing Using Native Consistent Hashing (CRUNCH)*, to maintain load balancing among the remaining active banks while providing efficient transitions.

Our paper makes the following contributions:

- To our knowledge, this is the first paper to observe and address the challenges of remapping data from powered-down banks in DRAM caches in a load-balanced manner, thereby *enabling dynamic DRAM cache resizing*.
- We propose a low-overhead mechanism, CRUNCH, to remap data from powered-down banks. Our mechanism, inspired by consistent hashing, incurs low latency/power overhead, while achieving good load balancing.
- We compare our mechanism, CRUNCH, to two data mapping schemes, one optimized for low transition overhead and the other optimized for load balancing. CRUNCH achieves the best of both worlds, resulting in both good steady-state performance and low transition costs.

## 2. Background and Motivation

In this section, we provide a brief characterization of application working set sizes, demonstrating the need for DRAM cache resizing. We then discuss DRAM cache organizations and two simple DRAM cache bank remapping schemes to illustrate the challenges in powering down DRAM cache banks.

### 2.1. Memory Footprint vs. Cache Capacity

Variations in working set sizes across applications, in addition to variations in cache activity across time (program phases), make it such that the full capacity of a DRAM cache is not always needed. Figure 1(a) shows the observed memory footprints for SPEC CPU2006 applications.<sup>1</sup> A few applications exhibit memory usage with large footprints that would benefit from large DRAM caches. However, in many other cases, the working sets would fit comfortably in a 128MB or smaller DRAM cache. Modern machines have multiple cores capable of simultaneously running multiple applications, and an effective DRAM cache should be able to accommodate the *aggregate* memory demands of multiple applications. Figure 1(b) shows the total working set sizes for all possible 4-core multi-programmed combinations of the SPEC2006 workloads. With multiple simultaneously-running applications, there is still a wide variance in memory demands, with

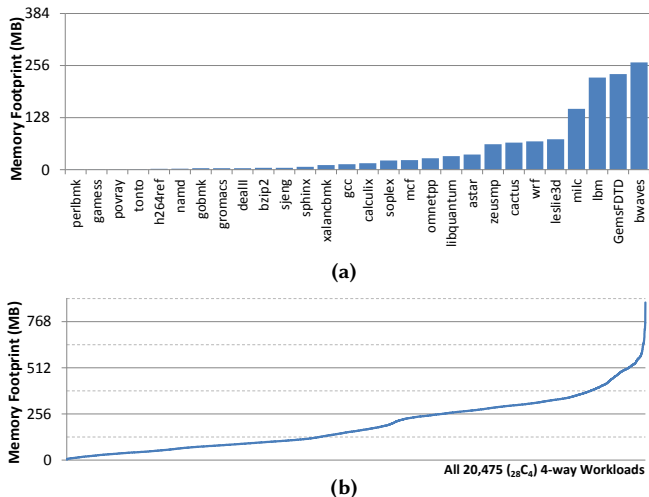


Figure 1: Memory footprints for (a) each of the SPEC CPU2006 applications, and (b) the aggregate footprint for each of the  $28C_4$  possible four-application multi-programmed workloads.

many combinations unable to fully utilize a large DRAM cache. For a 128MB DRAM cache, 44% of all 4-way workload combinations would use less than the full cache capacity; for a 256MB DRAM cache, 65% of the combinations do not use the full capacity. Therefore, although the generous capacity of die-stacked DRAM caches is beneficial for some workloads/applications, there clearly exist many scenarios where such a large cache is an overkill.

### 2.2. DRAM Cache Organizations

**SRAM Tag Store and Multi-Banked Cache Sets:** One simple approach to organize tags and data in a DRAM cache is to follow the conventional layout for a multi-banked SRAM cache as shown in Figure 2(a). This organization has a dedicated on-chip storage (i.e., SRAM) for tags<sup>2</sup> and it splits the data into multiple banks, thus each cache set is distributed across multiple banks for a set-associative cache. However, using an on-chip tag store incurs tens of MB of overhead due to the large projected capacities of DRAM caches [18, 23]. As a result, a conventional SRAM-style organization is impractical for implementing a DRAM cache.

**Tags in one DRAM bank and Multi-Banked Cache Sets:** To eliminate a large SRAM tag store, tags can be stored in one/more DRAM banks with data distributed across the remaining banks as shown in Figure 2(b). There are two main disadvantages with this organization. First, performance will suffer as the tag banks becomes a severe bottleneck, because *all* requests must access these banks for tag-lookup. Furthermore, DRAM cannot multi-port or pipeline accesses like SRAM does, because only one row may be opened at a time. Second, the power consumption increases linearly with the number of tags banks because each access now requires

<sup>1</sup>Simulation methodology is described in Section 4.

<sup>2</sup>A tag store can be single- or multi-banked.

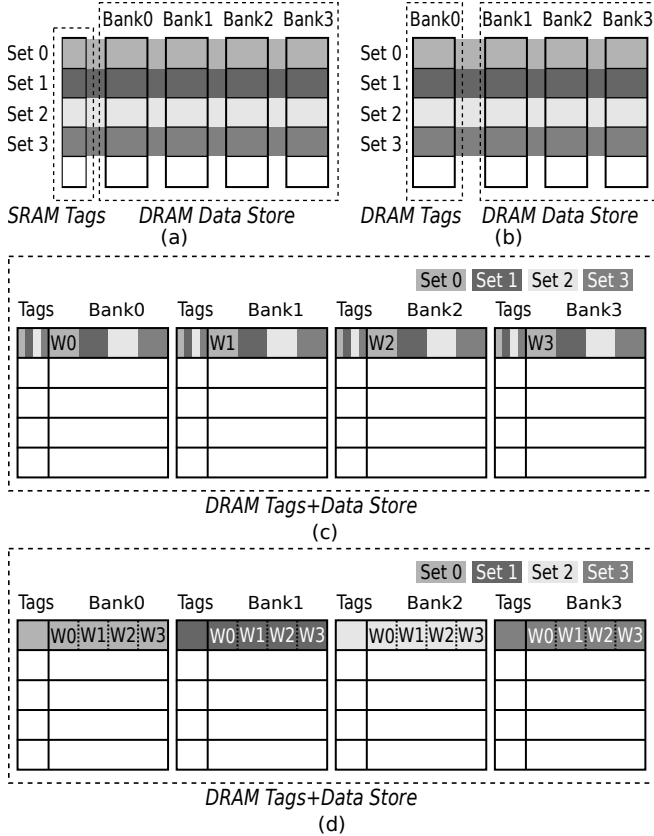


**Figure 2: Different tags and data organizations for DRAM caches:** (a) tags in SRAM and data in DRAM, (b) one dedicated DRAM bank for tags and the remaining banks for data, (c) tags in DRAM with sets distributed across banks, and (d) tags in DRAM with sets in a single bank. Each bank in (c) and (d) is the same as a bank in (a) and (b). They may appear different because we are showing a more detailed cache set-layout in (c) and (d).

activating multiple banks for tags and data.

**Tags in DRAM and Multi-Banked Cache Sets:** Another alternative to eliminate a large SRAM tag store is to store tags in the DRAM in the same row as their data. Figure 2(c) shows a DRAM cache using an SRAM-like layout with tags and data distributed across all banks. Using this organization has two main disadvantages. First, every cache line lookup requires accessing *all* banks in parallel, which significantly increases the dynamic power consumption. This is because every lookup requires sending one row activation to each bank. Second, the opportunity to serve multiple cache line lookups in parallel from different banks (i.e., bank-level parallelism [22]) reduces because *all* banks are required to serve one lookup.

**Tags in DRAM and Single-Banked Cache Sets:** To reduce the number of costly row activations required to perform an access, Loh and Hill [23] proposed the DRAM cache organization shown in Figure 2(d). This organization packs data and tags of a set together in the same physical DRAM row/page within a bank. Figure 3 shows the power con-

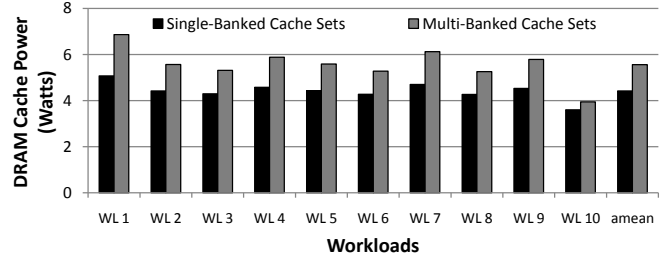


**Figure 3: DRAM cache power consumption comparison between the multi-banked cache sets design (shown in Figure 2(c)) and the single-banked cache sets design (shown in Figure 2(d)).**

sumption of DRAM caches with this organization and the multi-banked cache sets organization (shown in Figure 2(c)) across multiple workloads<sup>3</sup>. On average, the multi-banked design consumes 25.9% more power than the single-banked design proposed by Loh and Hill [23]<sup>4</sup>. Therefore, unless stated otherwise, we assume a DRAM cache organization proposed by Loh and Hill for the remainder of this paper.

### 2.3. DRAM Cache Resizing Challenges

Prior works have studied resizing caches based on shutting down ways or banks [2, 30, 32, 40]. However, there are two main challenges with dynamically resizing a DRAM cache. First, resizing a cache with the Loh and Hill cache organization by powering down banks introduces a set-indexing issue because turning off a bank takes away all sets from that powered-down bank. To avoid 100% miss rates for those requests that access cache sets in a powered-down bank, we need to *remap* these requests' addresses to active banks. Although using organizations that have sets distributed across multiple banks as shown in Figure 2(a), (b), and (c) does not have set-indexing issues for dynamically resized caches, these organizations are not practical for large DRAM caches as discussed in the previous sub-section. The second challenge is handling dirty data in powered-down banks, which must either be written to memory or migrated to other banks<sup>5</sup>. More data migration incurs more overhead. We now discuss two simple remapping schemes to illustrate these challenges.

### 2.4. Two Simple Bank Remapping Schemes

**Bank Fail-Over:** The first scheme is *Bank Fail-Over* (BFO), where cache lines mapped to bank  $i$  simply get remapped, or fail over, to the next available consecutive bank (with wrap-around). Figure 4(a) shows an example DRAM cache with four total banks with one bank turned off. Cache lines that map to bank 1 (which is off) are failed over to bank 2 (displaced sets are shown as dark blocks in the figure). Such fail-overs are easily computed by using the bank-selection bits from the address in conjunction with a vector that indicates which banks are active. In addition, because BFO

<sup>3</sup>Simulation methodology is described in Section 4.

<sup>4</sup>Although workload 10 has very low memory intensity (<2 L3-MPKI), it still increases the power by 9.3% when using the multi-banked cache sets design.

<sup>5</sup>Clean data can be safely dropped, which is what we assume in this paper.

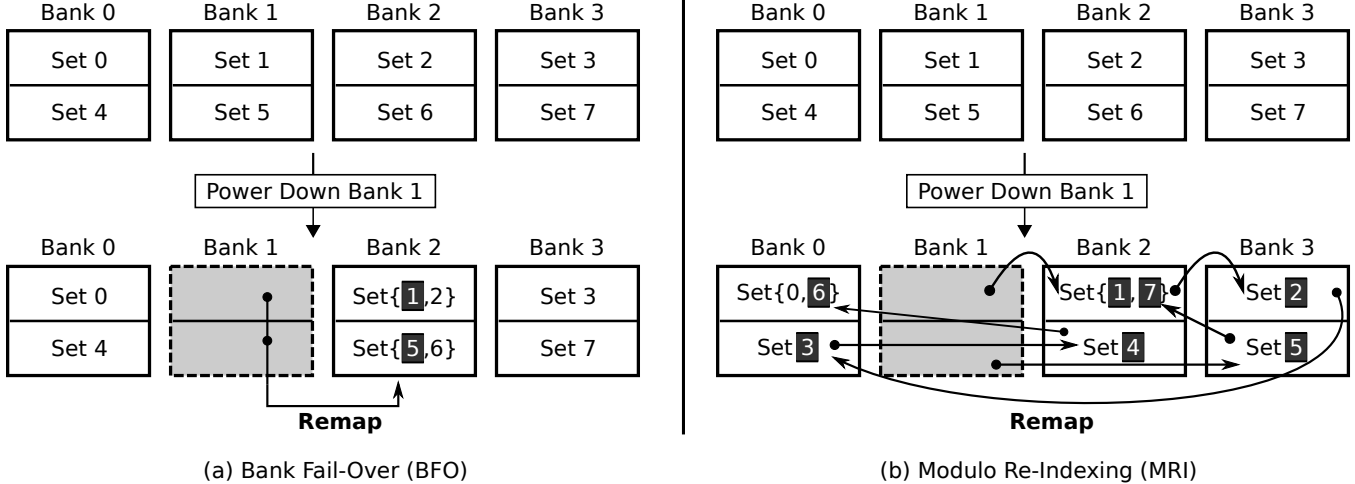


Figure 4: (a) An example scenario for Bank Fail-Over where cache lines mapped to a powered-down bank are remapped to the next sequential active bank. Dark blocks (white text) indicate sets that are remapped from one bank to another. (b) An example scenario for Modulo Re-Indexing where the address is reshaped (mod 3) and then remapped to a new bank.

allows addresses from multiple banks to be remapped to the same bank, the cache tags must be widened to include the bank-selection bits.

The advantage of BFO is that when a bank is turned off, *only cache lines in the powered-down bank are impacted*. In particular, BFO moves only dirty cache lines to the fail-over bank. In the worst case, a 100% dirty bank requires migration or writeback of all of its cache lines, but no other banks will be affected (apart from having to accept the incoming migrants).

The disadvantage of BFO is that after bank shut-down, there exists the potential for *unbalanced load distribution* across banks. For example in Figure 4(a), after bank 1 goes down, bank 2 has twice as much capacity pressure as the other banks from having to accommodate bank 1’s cache lines as well as those originally mapped to bank 2. This can lead to a sharp increase in conflict misses for the affected banks.

**Modulo Re-Indexing:** The second scheme, *Modulo Re-Indexing* (MRI), redistributes *all* cache lines evenly across the remaining banks. In the top of Figure 4(b), all four banks are on, and the bank index for a given line is computed by taking some number of bits from its physical address and performing a modulo-4 operation. With MRI, when there are only  $k$  banks enabled, we compute the bank index by performing a modulo- $k$  operation ( $k=3$  in this example) and then shifting the computed bank index to map to the actual enabled bank’s index. Other than the modulo computation hardware for re-indexing, MRI’s hardware requirements are similar to that of BFO (wider tags and bank selection from among enabled banks).

The advantage of MRI is that cache lines are uniformly redistributed across all banks, so no bank will be significantly more prone to being a hotspot than any other. The disadvantage is that  $k$  (number of active banks) changes as banks are powered-down or -up, thus the majority of cache lines

Scheme	Fast Transition Latency	Load Balancing
Bank Fail-Over	Yes	No
Modulo Re-Indexing	No	Yes
<b>CRUNCH</b>	<b>Yes</b>	<b>Yes</b>

Table 1: Summary of the strengths and weaknesses of the Bank Fail-Over and Modulo Re-Indexing schemes, along with CRUNCH proposed in this paper.

will be remapped to new banks *on every transition*. This global reshuffling of cache contents, while good for load balancing, severely increases the latency for powering down a bank, as nearly all dirty cache lines migrate to their newly assigned banks<sup>6</sup>. Thus, MRI’s power-down transition latency is proportional to the dirty data contained across *all* banks.

The descriptions above on power-down transition latency also apply to bank *power-up* transition latency. With BFO, dirty cache lines in the fail-over bank must be “repatriated” back to the bank that is being powered up. On the other hand, with MRI, cache lines from all of the banks must be re-shuffled using the updated modulo- $(k+1)$  mapping.

**Design Objective:** Each of BFO and MRI have their strengths and weaknesses, which are summarized in Table 1. BFO has bank power-down/up latency proportional to only the number of *powered-down* banks, but suffers from poor load-balancing. MRI achieves uniform load balancing, but suffers from poor transition latencies proportional to the *total* number of active banks. In this work, we propose *Cache Resizing Using Native Consistent Hashing* (CRUNCH), a new DRAM cache remapping scheme, to simultaneously achieve *both* fast transition latency and load-balanced cache line distribution.

<sup>6</sup>Alternatively, they can be written back to main memory, and then on the next miss reinstalled into the newly assigned bank.

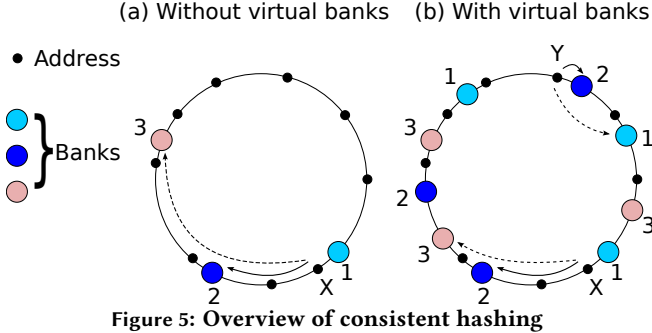


Figure 5: Overview of consistent hashing

### 3. Remapping via Native Consistent Hashing

The key challenges in remapping addresses to handle bank shut-down are (1) ensuring load-balanced address remapping and (2) achieving efficient dirty data migration. This section details how our design leverages key ideas from consistent hashing to handle the address remapping challenge and to correctly and efficiently migrate dirty data. Note that CRUNCH focuses on the remapping mechanism and can work with any cache sizing policy (e.g., [3, 30, 38, 40]).

#### 3.1. Consistent Hashing: A Brief Overview

Consistent hashing maps addresses to banks indirectly by first hashing both the banks and addresses on to the same unit circle. Each address maps to the first available bank encountered in a clockwise walk of the unit circle starting from its own hash-value on the unit circle. As shown in Figure 5(a), address X maps to bank 2 because it is the first bank encountered in a clockwise walk (see solid-arrow). If bank 2 were to be powered down, address X maps to the next bank in clockwise order, which is bank 3 (see dashed arrow). We define bank 3 to be the *fail-over* bank for bank 2 for address X. Note that in this example, any address that maps into the *region* of the unit circle between banks 1 and 2 (e.g., X) maps to bank 2, and subsequently fails over to bank 3 if bank 2 is disabled. As shown, this is identical to BFO. To provide load balancing, consistent hashing creates multiple *virtual banks* for each physical bank, such that each bank is actually associated with multiple regions distributed around the unit circle. For example, Figure 5(b) shows three copies of each bank. An address maps to a bank if it maps to any of the virtual copies of the same bank. Thus, both X and Y map to bank 2. Because the virtual bank copies are permuted in pseudorandom order by the hashing function, there is not one single fail-over bank for all addresses in bank 2. For example, the fail-over bank for address Y is bank 1 whereas the fail-over bank for address X is bank 3.

Because of symmetry, one can see that the properties are similarly true for bank power-up. Only a proportional fraction of addresses are remapped to a newly powered-up bank *and* the addresses that are remapped are distributed among all the previously active banks.

#### 3.2. Multi-namespace Variant

We develop a modified variant of the above consistent hashing mechanism that facilitates easier hardware implementa-

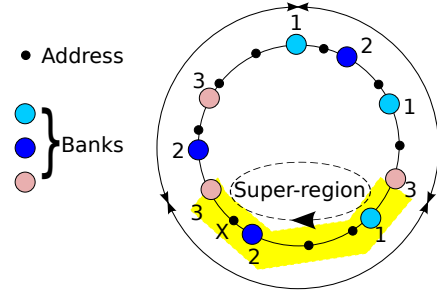


Figure 6: Multi-namespace variant of consistent hashing.

tion in CRUNCH, while retaining the basic design goals of load-balancing and minimal remapping. The modified variant introduces two changes in how addresses and resources (i.e., banks) are mapped to the unit circle. The first change decomposes the mapping of the addresses to the unit circle into a two stage-process: addresses are first mapped to “super-regions” of the unit-circle, and then they are further mapped to a region within the super-region. The second change replaces pseudo-random hashing of resource replicas with a more-careful construction. Under the original consistent hashing, resource distribution may have some non-uniformities. For example, there may be differences in distribution of the resource replicas with some parts of the unit circle having higher resource density than others. Similarly, it is also possible that multiple replicas of the same resource may be consecutive in clockwise order. We address this problem by artificially placing exactly one copy of each resource in each super-region. Consequently, each super-region has as many regions as resources. The exact order in which the resources/regions appear in the super-region is pseudo-randomly permuted. Figure 6 illustrates an example in which the unit circle is divided into three super-regions. Within each super-region, there is exactly one virtual instance of each bank. Further, we modify the fail-over strategy within a super-region to be limited to resources in that super-region. Thus, when an address exhausts all resources in a clockwise walk in a super-region, it wraps around to the first resource in the same super-region, as illustrated in Figure 6. The address X originally maps to bank 3. When bank 3 is unavailable, the address X would map to bank 2 in traditional consistent hashing because bank 2 appears next in a clockwise walk of the unit-circle. In our variant, the constraint on mapping within a super-region forces address X to wrap-around to the beginning of the super-region and thus maps to bank 1 instead.

#### 3.3. Remapping from a Shut-Down Bank

The CRUNCH hardware implementation of our consistent hashing variant uses a *region remapping table (RRT)* that contains the mapping from each region to each physical DRAM cache bank. We organize the RRT as a two-dimensional table as shown in Figure 7. Along the first dimension, the table holds rows corresponding to each super-region. Each

per-super-region row holds a wide word that contains a pseudorandom permutation of all banks.

The number of super-regions/regions is a design choice that affects load balance and table size. Because a region is the smallest unit of the address space that remaps to other banks, we are able to achieve better load balance with a larger number of smaller regions. However this may lead to a larger table. On the other hand, with a small number of regions, the RRT can be small and fast; but the remapping of regions to other banks occurs in chunks that may be too large to distribute evenly across all banks. Fortunately, this tension between remap granularity and table size is not a serious problem. Because the number of banks is typically small (say, 8 banks per channel), using 256 total regions (which corresponds to 32 super-regions) is sufficient to ensure good load balance. Our sensitivity studies with a larger number of regions (2048 regions in 256 super-regions) show that there is no significant benefit from larger RRTs.

Our design choices imply a 32-entry RRT where each entry contains 24 bits (8 bank-ids, each of which is 3-bits wide) for a total of 96 bytes, which is small compared to the DRAM cache. Furthermore, the RRT table does not change the DRAM internals and it is implemented in the DRAM cache controller. Note, the RRT is a read-only table which contains pseudorandom permutations of the bank-ids. Because it is read-only, it may be computed statically using arbitrary algorithms at design time. Furthermore, the problem sizes are fairly small for offline analysis; we have to choose 32 permutations that are not rotation equivalent (for our 32-entry RRT) out of 5040 ( $= 8!/8 = 7!$ ) possible permutations. Ideally, the permutations must be chosen carefully such that the fail-over banks are balanced for any number and combination of banks being shut-down. However, we use a simpler method in which we only ensure that the fail-over banks are evenly distributed with one bank failure. Our results show that our simple table generation method achieves performance very similar to MRI, which perfectly load balances the different sets across banks, and so we do not believe that there is significant value in further optimizing the fail-over orders.

Each access to the DRAM cache first maps the address to the appropriate bank by consulting the RRT. When all banks are active, the appropriate bank is selected from the permutation by first indexing into the RRT to read the appropriate super-region entry; and then selecting the bank by using the additional bits of the region-index. When some banks are inactive, we do a priority-selection to find the first active bank in permutation order within the super-region. Because RRT lookup is at hardware speeds, DRAM cache access latency remains comparable to traditional bank-selection latency, which typically uses simpler forms of hashing ranging from trivial bit-selection to bit “swizzling” techniques.

### 3.4. Handling Dirty Data in a Shut-Down Bank

When shutting down a bank, dirty data in the bank must be handled correctly. One simple approach writes back all dirty

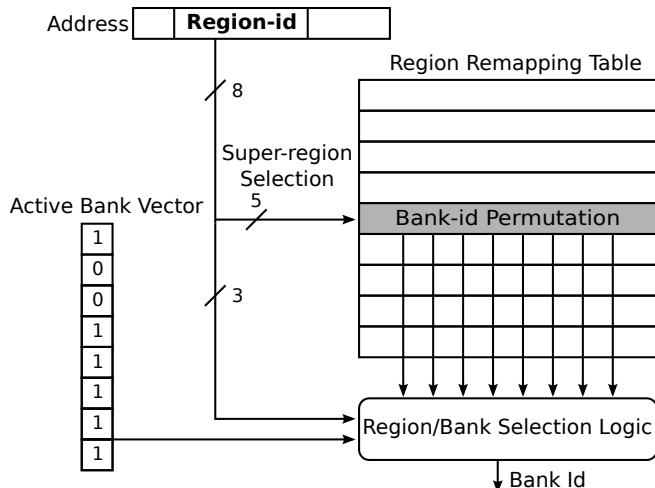


Figure 7: CRUNCH hardware

lines to main memory. We employ an alternative approach that migrates the data from its home bank (i.e., the bank under the old mapping) to its new bank. Such migration retains some data in the DRAM cache while ensuring that dirty data is not “lost” to subsequent reads<sup>7</sup>. The motivation for migrating (as opposed to writing back) is that write-back operations are limited by the off-chip memory bandwidth, while migration between banks can use the DRAM cache’s larger bandwidth. Note that there might be a case where migrating some clean data (e.g., top-N MRU lines) is beneficial for the steady-state performance (despite an increase in the transition latency). We leave this as part of future work.

### 3.5. Finding the Dirty Blocks

The need to writeback/migrate all dirty data in a DRAM cache bank requires the enumeration of all dirty blocks. While the dirty bit in traditional write-back cache designs can identify a given block as dirty/clean, it cannot offer an efficient *enumeration* of dirty blocks for writeback or migration. A naive implementation, based on a full walk of the cache bank to identify and enumerate dirty data, incurs cost proportional to the size of cache banks even in cases where the amount of dirty data is a small subset of the data in the cache bank.

We develop an improved implementation with hierarchical dirty bits (HIER) in which a tree-based hierarchy of dirty row counters indicates dirty-block presence at successively coarser-grain collections of DRAM rows. For example, a root-level dirty block counter indicates the number of rows in the entire DRAM cache that have at least one dirty block. At the next level of the tree, a set of  $d$  dirty row counters indicate the number of rows in each of the  $\frac{1}{d}$  fractions of the DRAM cache that hold dirty blocks. The hierarchy ultimately terminates at the individual DRAM cache rows. Such a hierarchy enables pruning of the cache walk by avoiding coarse-grain regions

<sup>7</sup>Strictly speaking, correctness is not affected if lost data is (transitively) dynamically dead. However, we adopt a strict definition of correctness in which any lost data is treated as a violation of correctness.

of cache that hold clean data.

HIER incurs two overheads; one in space and the other in time. The space overhead is modest because we only count rows that hold dirty blocks as opposed to the dirty blocks themselves. HIER uses a perfectly-balanced  $d$ -ary tree that is easy to represent in linear arrays (similar to  $d$ -ary heaps). The number of entries needed to handle  $R$  rows is approximately  $(d \cdot R)/(d - 1)$  counters. For example, consider an  $R=2,048$ -row DRAM cache bank, with  $d = 16$ . The root counter must be 12 bits wide to count up to 2,048 dirty rows. The leaf-node counters, however, are only 1 bit wide to indicate whether there are any dirty blocks within each respective row. Counters at intermediate nodes in the tree are sized appropriately to count the number of rows covered within that super-region. This amounts to only 2,772 bits (346.5 bytes) per table per bank. Assuming eight banks per channel, and four channels per DRAM stack (see Section 4), this adds up to 10.8KB for a 128MB DRAM cache. Note that HIER is not solely used for CRUNCH, but it is also used for BFO and MRI, incurring the same overhead for all mapping schemes. As we will show in the evaluation section, HIER provides significant benefit to all remapping schemes.

The HIER structure is implemented as a small SRAM table alongside the DRAM cache controller and remapping logic. When a row’s dirty counter changes from dirty to clean (or vice versa), the changes need to be propagated up the tree to the root. This propagation delay is a negligible time overhead because (1)  $d$ -ary trees are fairly shallow, (2) access times to small SRAM arrays are short compared to DRAM cache access times, and (3) the propagation is not on the critical path for the main DRAM cache accesses.

### 3.6. Repatriating Displaced Dirty Blocks

A powered-down bank’s dirty data may be displaced to several (potentially all) active banks. When that bank is eventually powered up, all its displaced data has to be brought back to the newly powered-up bank. This need for dirty-data repatriation imposes two costs; discovery costs to locate such remote dirty data, and migration costs to copy the data over to the newly powered-up bank.

To discover dirty data with CRUNCH and MRI, a naive approach is to walk all banks to discover remote dirty blocks (with HIER optimizations to expedite the cache walks). An alternative is to disallow remote blocks from being dirty (i.e., write-through for these blocks only). However, this may result in steady-state costs in the form of higher write-traffic to main memory because of write-through blocks. Because this design increases steady-state cost to reduce the (uncommon) transient costs, we do not consider this design in this paper. On the other hand, BFO has an advantage because all displaced dirty blocks that need to be repatriated can be found in exactly one fail-over bank.

Processor	4-core, 3.2 GHz, 4-wide issue, 256 ROB
Private L1 cache	4-way associative, 32 KB
Shared L2 cache	16-way associative, 4 MB
Stacked DRAM cache	29-way associative [23], 128 MB, 1 GHz (DDR 2 GHz), 128-bit channel, channels/ranks/banks = 4/1/8, 2 KB rows, tCAS/trCD/trP = 8/8/15
Off-chip DRAM	8 GB, 800 MHz (DDR3 1.6 GHz [28]), 64-bit channel, channels/ranks/banks = 2/1/8, 2 KB rows, tCAS/trCD/trP = 11/11/11

Table 2: Configuration of simulated system.

## 4. Experimental Methodology

**Simulator Model:** We use MacSim [15], a cycle-level x86 CMP simulator for our evaluations of application-level performance. We model a quad-core CMP system with private L1 caches, and a shared L2 cache. We use a detailed DRAM timing model for the shared L3 *stacked DRAM* cache and the off-chip main memory (DDR3 SDRAM-1600 [28]). Unless stated otherwise, our detailed system configuration is as shown in Table 2. The size of our DRAM cache is 128 MB. As we discussed in Section 2.2, we assume the DRAM cache organization proposed by Loh and Hill [23].

**Power Model:** We modified Micron’s DRAM power calculator [27] to estimate the DRAM cache power. In contrast to off-chip DDR3, stacked DRAM has a much wider data width of 128 bits. Hence, only one stacked DRAM chip is accessed for each read or write command, as opposed to eight chips in the case of x8 DDR3. The stacked DRAM therefore requires less energy per activation because it does not need to access duplicate sets of peripheral circuits (e.g., row decoders), although we assume the actual read/write energy itself remains the same because the same total number of bits are driven. The DRAM power calculator’s IDD values are adjusted accordingly. Furthermore, we double stacked DRAM’s refresh rate to factor in the higher operating temperature [9].

**Workloads:** We evaluate our system using SPEC CPU2006 [36]. We focus on memory-intensive benchmarks because the DRAM cache has very little impact on low memory-intensity applications. To form suitable workloads, we group the benchmarks into categories based on L2 misses per thousand instructions (MPKI). Benchmarks with MPKI > 25 are in Category H (high intensity), while those with MPKI > 15 are in Category M (medium intensity), and the rest of the benchmarks are in Category L (low intensity). We construct 10 multiprogrammed workloads using these benchmarks, as shown in Table 3, for our main evaluations.

**Evaluating Different Data Remapping Schemes:** To evaluate the effects of different data remapping schemes on power and performance, we would ideally like to run *seconds*-long simulations where banks are powered up and down dynamically, with data being remapped on every transition. However, the cycle-level simulation time would be

Mix	Workloads	Category
WL-1	mcf mcf mcf mcf	4H
WL-2	mcf lbm milc libquantum	4H
WL-3	libquantum mcf milc leslie3d	4H
WL-4	milc leslie3d libquantum milc	4H
WL-5	libquantum milc astar wrf	2H+2M
WL-6	milc mcf soplex bwaves	2H+2M
WL-7	milc leslie3d GemsFDTD astar	2H+2M
WL-8	libquantum bwaves wrf astar	1H+3M
WL-9	bwaves wrf soplex GemsFDTD	4M
WL-10	gcc gcc gcc gcc	4L

Table 3: Multiprogrammed workloads.

prohibitive with such an approach and the benefits/trade-offs of different remapping schemes can be evaluated without such a full-scale evaluation. Therefore, we decouple the simulation to separately evaluate the different aspects of the data remapping schemes. This methodology is similar to those in other studies for evaluating scenarios spanning much longer timescales than typical cycle-level simulation sample sizes [24].

First, we evaluate system performance of different remapping schemes when different numbers of banks are turned on. This allows us to examine the performance impact of each remapping scheme’s cache line distribution (load balancing) with a specific bank configuration, for a certain length of time. We call this the *steady state* analysis. For evaluating each scheme, we use a specific number of shut-down banks and simulate 100 million instructions per benchmark. We gather statistics for each benchmark once it retires 100 million instructions. Simulation of all benchmarks continues (to continue to contend for the memory system) until each one has executed 100 million instructions.

Second, we evaluate different remapping schemes based on the transition latency and energy overheads, which we call the *transition* analysis. We carry out this analysis by first warming up the DRAM cache with all banks enabled (for the power down study) or a specified number of banks disabled (for the power up study). Once the warm-up completes, we power down (or up) banks, and measure the latency of the transition and the energy expended to remap dirty blocks. We run each simulation for 150 million warm-up cycles, and then execute until the transition completes.

Third, we generate a representative set of patterns for shutting down banks instead of using all possible combinations. A policy that determines how many and which banks to power-up/down is beyond the scope of this paper as we focus on the remapping problem. Table 4 shows the patterns for our evaluations. For each pattern, bank index starts from left (bank 0) to right (bank 7). The number at each index indicates if the bank is turned on (1) or off (0). We use a “binary search” approach for selecting bank shut-down order to avoid (as much as possible) pathological cases where a large number of shut-down banks all fail-over to the same bank in BFO, thereby creating an unfairly severe hotspot.

Number of Shut-down Banks	Shut-down Pattern
1	11110111
2	11010111
3	11010101
4	10010101
5	10010001
6	10000001
7	10000000

Table 4: Bank Shut-down Patterns.

We later show in Section 5.5 that CRUNCH is robust against different bank shut-down patterns.

**Performance Metrics:** For the steady-state analysis, we report system performance using the *Weighted Speedup* metric:

$$WeightedSpeedup = \sum_{i=1}^N \frac{IPC_i^{shared}}{IPC_i^{alone}} \quad [8, 35]$$

For the transition analysis, we report the latency of powering up and down banks in *cycles*. We also report DRAM energy consumption during power-up/down transitions.

## 5. Experimental Evaluation

### 5.1. Steady-State System Performance

In this section, we evaluate the impact of different remapping schemes on system performance in terms *weighted speedup* during steady state operation. Specifically, we shut down different numbers of banks and examine the load-balancing effect of each remapping scheme. Figure 8 shows the steady-state system performance of each remapping scheme averaged (geometric mean) across all workloads for different numbers of active banks. We draw two key conclusions.

First, CRUNCH, with carefully designed region remapping tables, provides performance comparable to MRI. Therefore, we conclude that CRUNCH achieves good load balancing, on par with MRI. In fact, except for the case of three enabled banks, CRUNCH provides slightly better average system performance than MRI. While MRI provides even distribution over the address space, the simple *modulo-k* mapping means that accesses at strides that are not relatively prime to the number of enabled banks will map to a restricted subset of the available banks. In contrast, the RRT lookup in CRUNCH performs a swizzling that will evenly distribute these strided accesses across all available banks. As a result, we expect that MRI coupled with a reasonable swizzling scheme would perform on par with CRUNCH in the steady state.

Second, CRUNCH outperforms BFO when at least one bank is powered down. This is because BFO creates unbalanced load distribution by remapping all cache lines within a powered-down bank to the next available consecutive bank. For instance, when one bank is powered down, the consecutive bank will receive roughly twice as much request traffic as the other remaining banks. To quantitatively compare the load balancing effect between different remapping schemes, we define a metric called the *imbalance ratio*. The imbalance ratio is the maximum request traffic to any bank divided by the minimum request traffic to any other bank.



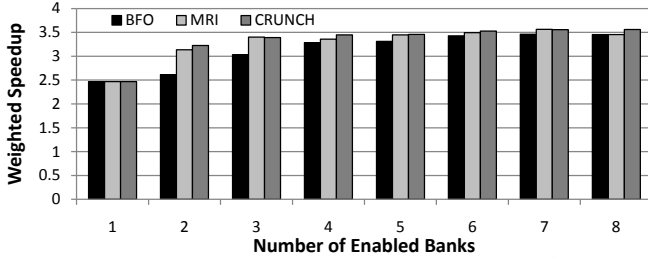


Figure 8: Steady-state system performance (weighted speedup) of the evaluated bank remapping schemes across varying numbers of enabled DRAM cache banks.

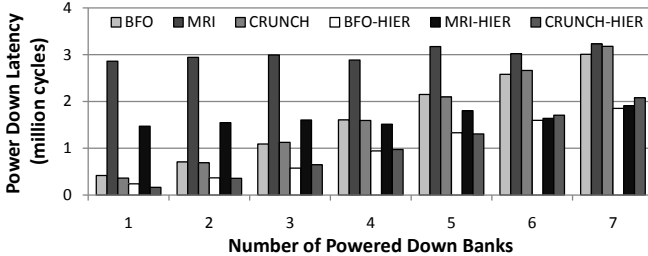


Figure 9: The power-down transition latencies of remapping schemes for varied numbers of powered-down banks.

With three active banks, we observe the imbalance ratios are 4.2, 1.3, and 1.0 for BFO, CRUNCH, and MRI, respectively, on average across all workloads. The high bank imbalance leads BFO to reduce average system performance by 11% compared to CRUNCH. In summary, CRUNCH provides the ability to consistently provide low imbalance ratios, enabling high system performance, for all workloads. Thus, we conclude that CRUNCH achieves the design goal of effectively load-balancing cache line distribution across banks.

## 5.2. Power-Down Transition Analysis

**Latency Analysis:** There are two phases in powering down a cache bank. The first phase is searching the bank for all modified cache lines so that they can either be migrated to another bank or written back to main memory. The second phase is actually performing the data transfer. The latency associated with performing these operations is a factor in system performance as well as in determining how responsive a power management scheme can be to short-term changes in workload behavior.

Figure 9 shows the power-down transition latency averaged across all evaluated workloads for shutting down different numbers of banks (starting with all eight banks enabled), with and without the proposed hierarchical dirty bits technique (HIER). Two conclusions are in order. First, CRUNCH achieves significantly lower power-down latencies than MRI, on par with BFO. Second, as the number of powered-down banks decreases, the transition latency also drops for CRUNCH and BFO, whereas the transition latency remains approximately the same for MRI. This is because CRUNCH and BFO only need to walk through and transfer dirty cache lines in the powered-down banks. In contrast, MRI requires walking through all banks because *all* cache

lines are remapped across the remaining active banks after banks are powered down.

**Effect of hierarchical dirty bits:** Figure 9 shows that using the proposed hierarchical dirty bits technique (HIER) provides consistent latency reductions for all workloads and variations of powered-down bank counts, with maximum reductions of 49%, 55%, and 49% for BFO, CRUNCH, and MRI, respectively. This is because using HIER avoids unnecessary cache walks by enumerating dirty lines directly for migrations.

**Transition impact on instantaneous performance:** To gain a better sense of how the power-down transition impacts instantaneous performance and system responsiveness, Figure 10 and Figure 11 show detailed performance traces sampled over time for two representative workloads, WL-1 and WL-2, when shutting down two banks. The y-axis indicates the total number of retired instructions during the last sampling period (500K cycles). Several conclusions can be drawn from this data.

First, the system performance drops significantly regardless of the remapping schemes used for both workloads. The reason is that the DRAM cache is prevented from servicing memory requests during the transition to guarantee correctness.

Second, MRI has a much larger transition latency than both BFO and CRUNCH. There are two main reasons for this. First, MRI requires walking through the whole cache to enumerate dirty cache lines because cache lines are uniformly distributed across all active banks. Second, MRI also needs to migrate more dirty cache lines than BFO and CRUNCH because of the same explanation as the first reason: uniform cache line redistribution. For instance, the number of migrated dirty cache lines are 817, 842, and 2606, for BFO, CRUNCH, and MRI, respectively, for WL-1’s example transition in Figure 10. As a result, the migration latency is significantly higher for MRI. In addition, MRI provides lower system performance during the initial program phase right after the completion of power-down transitions for both WL-1 and WL-2. For example, Figure 10 clearly shows that the retired instruction curve for MRI falls below BFO and CRUNCH after the transition completes at the sample point 305. This occurs because MRI remaps a large number of clean cache lines. Therefore, most of the requests will result in misses during the program phase after the completion of power-down transitions.

Third, the transition overhead for WL-2 is greater than that for WL-1 simply because WL-2 has a much larger quantity of dirty data, thus requiring longer latency for transferring these dirty cache lines. For WL-2, the number of migrated dirty cache lines are 134937, 120630, and 393366, for BFO, CRUNCH, and MRI, respectively, which is at least 100x more than WL-1.

**Energy Analysis:** Figure 12 shows the energy consumption for each remapping scheme with HIER applied as the

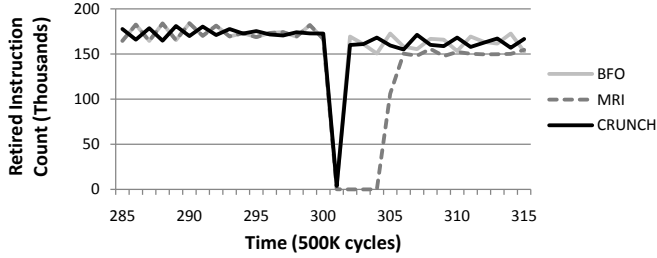


Figure 10: Performance of WL-1 sampled over time.

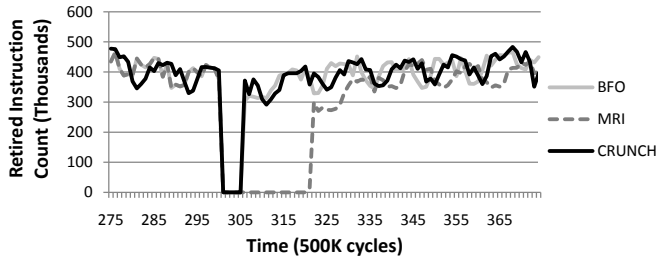


Figure 11: Performance of WL-2 sampled over time.

number of powered-down banks is varied. Because energy consumption is proportional to the number of dirty cache line migrations, the energy numbers follow the same trend as the latency numbers. The following are some major conclusions. First, BFO and CRUNCH consume significantly lower energy for lower numbers of powered-down banks, as they need to migrate only the dirty cache lines in the powered-down banks. On the other hand, MRI’s power consumption remains roughly the same for all bank configurations because MRI remaps data in *all* banks. Second, CRUNCH actually consumes 3.8% and 8.8% more energy than MRI when shutting down six and seven banks, respectively. This is because CRUNCH needs to migrate 3.6% and 7.6% more dirty lines when shutting down six and seven banks respectively, than MRI for these two configurations. Nonetheless, CRUNCH consumes 8.6x less energy than MRI in the best case (shutting down one bank).

### 5.3. Power-Up Transition Analysis

**Latency Analysis:** Powering a cache bank back up requires finding all of the modified cache lines that previously would have mapped to this bank, but were displaced elsewhere. This requires searching one or more banks, and then either repatriating those cache lines back to this bank, or writing them back to main memory. Figure 13 shows the power-up transition latency (when powering back up to all eight banks enabled) averaged across all evaluated workloads for different remapping schemes along with the HIER mechanism. We draw the following conclusions.

First, using BFO consistently provides lower transition latency for powering up banks, compared to both CRUNCH and MRI across all variations of powered-up bank counts. As explained in Section 3.6, this is because BFO only needs to search through a subset of active banks that contain failed-over cache lines. Finding these active banks is straightforward because they are the next sequential active bank(s)

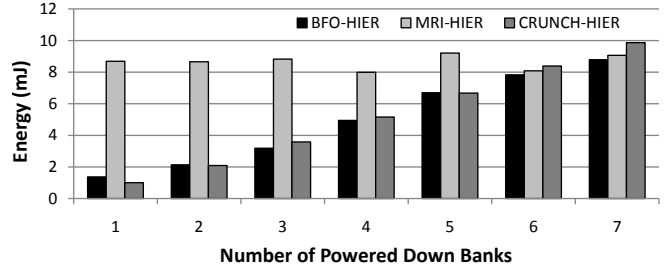


Figure 12: Energy consumption during power-down transitions

relative to the newly powered-up bank(s). On the other hand, both CRUNCH and MRI require searching every active bank to find the displaced dirty cache lines. As a result, when a naive cache line walking scheme that reads all cache lines in all active banks is employed, the latency of reading every cache line in the active banks to find displaced dirty bits dominates the transition latency for CRUNCH and MRI.

Second, similar to our observations for the power-down transition analysis, using a smarter cache line walking scheme (HIER) reduces the transition latency significantly for all remapping schemes. The maximum reductions are 66.2%, 69.3%, and 66.2% for BFO, CRUNCH, and MRI, respectively.

**Energy Analysis:** Figure 14 shows the energy consumption for each remapping scheme with HIER applied, as the number of powered-up banks is varied. Following are our key conclusions. First, the energy consumption is proportional to the transition latency as explained before, for powering down banks. Second, CRUNCH consumes less energy than MRI for all bank configurations since MRI requires remapping all data when the bank configuration changes. Third, BFO consistently provides lower energy consumption than both CRUNCH and MRI. This behavior is the same as for transition latency, which we explain in detail above. Nevertheless, CRUNCH provides better system performance than BFO during steady-state.

Although BFO provides the lowest power-up transition latency and hence transition energy among all the remapping schemes, as demonstrated in Section 5.1, it has the disadvantage of leading to potentially unbalanced cache line distribution, causing some banks to become hotspots and hence become bottlenecks for memory requests to these banks. Therefore, BFO’s lower power-up latency comes at the cost of reduced steady-state system performance. In contrast, CRUNCH not only provides high system performance with load-balanced distribution of cache lines, but it also enables fast transition latency for powering down banks and offers lower power-up transition latency than MRI. By applying a simple optimization, hierarchical dirty bits (HIER), the power-up transition latency gap between BFO and CRUNCH significantly reduces. In addition, other optimizations that can more efficiently enumerate dirty data or bound the amount of dirty data in the cache, could potentially further reduce the transition latency gap between BFO and

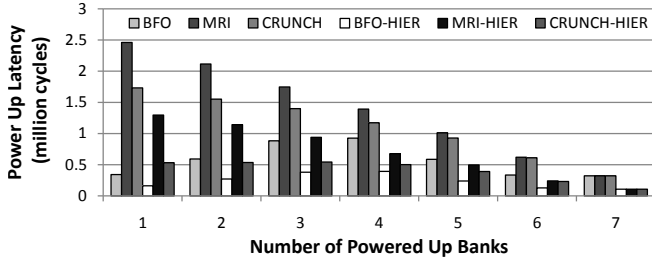


Figure 13: The power-up transition latencies of different remapping schemes averaged across all workloads for turning on different numbers of banks.

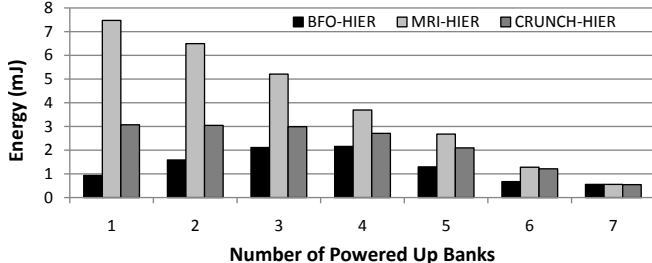


Figure 14: Energy consumption during power-up transitions CRUNCH. Therefore, we conclude that CRUNCH achieves the two design goals of enabling low transition latency and providing load-balanced cache line distribution.

#### 5.4. Sensitivity to System Parameters

**Varying Core Count:** Figure 15 shows the average steady-state system performance of different remapping schemes on an 8-core system running eight randomly-picked multiprogrammed workloads. Similar to the observation we made for our baseline 4-core system in Section 5.1, CRUNCH provides slightly better system performance than MRI and continues to outperform BFO. Therefore, we conclude that CRUNCH continues to provide both good steady-state performance and low transition latency/energy with increasing cache pressure.

#### 5.5. Impact of Sequential Bank Shut Down

In this section, we evaluate the impact of different bank shut-down patterns on steady-state system performance. For our evaluations so far, we have been using balanced bank shut-down patterns, described in Section 4. Alternatively, we can power down banks sequentially starting from the bank with the lowest index value. Figure 16 shows the steady-state performance comparisons between sequential and balanced bank shut-down orders. We make the following observations. First, BFO significantly reduces system performance when banks are being turned off sequentially. This is because BFO creates an unbalanced load distribution by remapping all the cache lines within the shut-down banks to a single active bank. Second, CRUNCH provides the same system performance compared to that of using balanced shut-down orders even if banks are sequentially disabled. The importance of

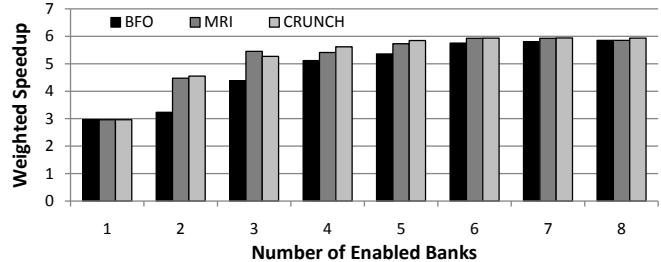


Figure 15: System performance of different remapping schemes on an 8-core system.

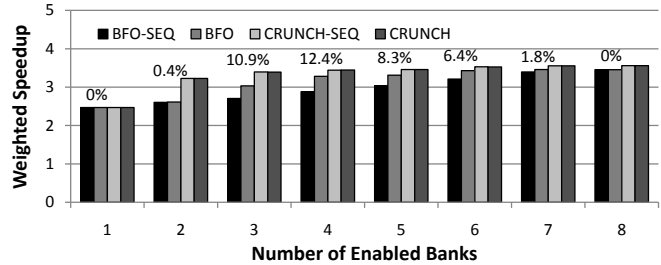


Figure 16: Steady-state performance comparisons between sequential- and balanced-order bank shut-down for BFO and CRUNCH. % values are performance degradations of BFO-SEQ relative to BFO.

these results is that with CRUNCH, the overall DRAM cache power management policy can be simplified so that it needs only figure out the *number* of banks that should be turned on, rather than which *specific* banks.

## 6. Related Work

While techniques to turn off banks have been studied by several works in the context of SRAM caches, the organization of DRAM caches poses additional challenges. Specifically, entire sets are mapped to a row in a bank. Therefore, powering down banks requires (1) remapping of the sets, mapped to the being powered-down banks, to the active banks and (2) migration of dirty data from the being powered-down banks to the active banks. Naive schemes to perform this remapping/migration suffer from the problem of either high transition times (to remap/migrate) or degrade performance in the steady state (after remapping/migration).

To our knowledge, this is the first work to propose a data remapping scheme that achieves both good load-balancing in the steady state and low bank power-up/down transition latency/energy.

A number of prior works have proposed to save SRAM cache power by disabling cache ways (e.g., [2, 32, 40]). Specifically, Albonesi [2] proposes to selectively disable cache ways in the L1 data cache to reduce dynamic power consumption. Bardine et al. [3] propose a D-NUCA cache that dynamically turns on/off ways based on the running application’s behavior, to save both dynamic and static power. Zhang et al. [40] propose a configurable cache design that allows varying the

associativity to save dynamic power.

Industry processors have also adapted dynamic cache sizing techniques to reduce leakage power. The Intel Core Duo Processor [30] implements a dynamically sizeable L2 cache which is down when the processor core enters deep sleep states. Similarly, AMD’s Steamroller processor [34] implements L2 cache resizing based on the workload. Both of these implementations disable ways of the cache to achieve a smaller size.

All of these works focus on small SRAM cache designs that have separate tag stores and whose ways are distributed across all banks. Therefore, turning off banks merely reduces the associativity of the cache. Our work, on the other hand, focuses on a large DRAM cache, for which a practical organization requires an entire set to be mapped to a row in a bank, as described in Section 2.2. Therefore, when turning off banks in such DRAM caches, the sets mapped to a bank need to be remapped to other active banks.

Prior works have proposed to dynamically adapt the cache size at a finer granularity by disabling cache lines using decay-based techniques (e.g., [1, 11, 12, 16, 20, 29, 41]). These are complementary to our proposed bank shut-down scheme and can be applied to DRAM caches as well.

Yang et al. [39] propose a hybrid technique that dynamically resizes caches to save leakage power by changing the number of active cache sets [33, 38] or ways [2]. Following are the key reasons why CRUNCH is significantly different from this work. First, this mechanism only allows power-of-two resizing in order to address the indexing issue when enabling or disabling sets. This scheme is similar to MRI with a power-of-two resizing and would result in a large number of misses, since a number of cache blocks would have to be remapped. Second, the mechanism’s primary focus is a policy to determine the number of sets or ways to dynamically resize, which is not the focus of our work.

There has also been significant work in reducing power in off-chip DRAMs (e.g., [5, 6, 13, 17, 37]). These works employ different techniques such as partial activation of the DRAM array or low energy operating modes to reduce DRAM power and do not address the challenges in turning off banks when DRAM is used as a cache.

## 7. Conclusion

Die-stacking technologies enable stacking a processor with DRAM and this DRAM can act as a large, high-bandwidth cache. While some workloads utilize the entire capacity of this large DRAM cache, several workloads use only a subset of this cache. Therefore, powering down banks of this DRAM cache can enable power savings, without degrading performance significantly. However, since entire sets are mapped to the same row (in a bank) in a typical DRAM cache, when a bank is powered down, the sets mapped to it need to be remapped to other active banks. Our goal in this work is to address this data remapping challenge, thereby enabling

DRAM cache resizing. To this end, we presented Cache Resizing Using Native Consistent Hashing (CRUNCH), a data remapping scheme that achieves both low transition latency *and* load-balanced cache line distribution. CRUNCH outperforms two state-of-the-art remapping schemes, providing *both* (1) high system performance during steady-state operation, with a certain number of banks turned on and (2) fast transition latency and energy when banks are powered up or down. Therefore, we conclude that CRUNCH provides an effective data remapping substrate, enabling DRAM cache resizing.

## References

- [1] J. Abella *et al.*, “IATAC: A smart predictor to turn-off L2 cache lines,” *TACO*, vol. 2, no. 1, pp. 55–77, March 2005.
- [2] D. H. Albonesi, “Selective cache ways: On-demand cache resource allocation,” in *MICRO-32*, 1999.
- [3] A. Bardine *et al.*, “Improving power efficiency of D-NUCA caches,” *ACM SIGARCH Computer Architecture News*, September 2007.
- [4] B. Black *et al.*, “Die-stacking (3D) microarchitecture,” in *MICRO-39*, 2006.
- [5] E. Cooper-Balis and B. Jacob, “Fine-grained activation for power reduction in DRAM,” *IEEE Micro*, vol. 30, pp. 34–37, 2010.
- [6] V. Delaluz *et al.*, “DRAM energy management using software and hardware directed power model control,” in *HPCA-7*, 2001.
- [7] X. Dong *et al.*, “Simple but effective heterogeneous main memory with on-chip memory controller support,” in *SC*, 2010.
- [8] S. Eyerman *et al.*, “System-level performance metrics for multiprogram workloads,” *IEEE Micro*, vol. 28, pp. 42–53, May 2008.
- [9] M. Ghosh and H.-H. S. Lee, “Smart refresh: An enhanced memory controller design for reducing energy in conventional and 3D die-stacked DRAMs,” in *MICRO-40*, 2007.
- [10] S. H. Gunther *et al.*, “Energy-efficient computing: Power management system on the Nehalem family of processors,” *Intel Technology Journal*, vol. 14, no. 3, 2012.
- [11] H. Hanson *et al.*, “Static energy reduction techniques for microprocessor caches,” *IEEE Transactions on VLSI*, vol. 11, pp. 303–313, 2003.
- [12] H. Hanson *et al.*, “Static energy reduction techniques for microprocessor caches,” in *ICCD*, 2001.
- [13] A. Hegde *et al.*, “VL-CDRAM: variable line sized cached DRAMs,” in *CODES+ISSS*, 2003.
- [14] U. Höelzle and L. A. Barroso, *The Datacenter as a Computer: An Introduction to the Design of Warehouse-Scale Machines*. Morgan & Claypool, 2009.
- [15] HPArch, “Macsim simulator,” <http://code.google.com/p/macsim/>.
- [16] Z. Hu *et al.*, “Let caches decay: reducing leakage energy via exploitation of cache generational behavior,” *TOCS*, vol. 20, pp. 161–190, 2002.
- [17] I. Hur and C. Lin, “A comprehensive approach to DRAM power management,” in *HPCA-14*, 2008.
- [18] X. Jiang *et al.*, “CHOP: Adaptive filter-based DRAM caching for CMP server platforms,” in *HPCA-16*, 2010.
- [19] D. Karger *et al.*, “Consistent hashing and random trees: Distributed caching protocols for relieving hot spots on the world wide web,” in *STOC-29*, 1997.
- [20] S. Kaxiras *et al.*, “Cache decay: Exploiting generational behavior to reduce cache leakage power,” in *ISCA-28*, 2001.
- [21] J.-S. Kim *et al.*, “A 1.2v 12.8gb/s 2gb mobile Wide-I/O DRAM with 4x128 I/Os using TSV-based stacking,” in *ISSCC*, 2011.
- [22] Y. Kim *et al.*, “Thread cluster memory scheduling: Exploiting differences in memory access behavior,” in *MICRO-43*, 2010.
- [23] G. H. Loh and M. D. Hill, “Supporting very large caches with conventional block sizes,” in *MICRO-44*, 2011.
- [24] M. R. Marty and M. D. Hill, “Virtual hierarchies to support server consolidation,” *ISCA-34*, 2007.
- [25] D. Meisner, B. T. Gold, and T. F. Wenisch, “PowerNap: Eliminating server idle power,” in *ASPLOS-14*, 2009.

- [26] J. Meza *et al.*, "Enabling efficient and scalable hybrid memories using fine-granularity DRAM cache management," *IEEE CAL*, 2012.
- [27] Micron Technology, "Calculating memory system power for DDR3," 2007.
- [28] Micron Technology, "4Gb: x4, x8, x16 DDR3 SDRAM," 2011.
- [29] M. Monchiero *et al.*, "Using coherence information and decay techniques to optimize l2 cache leakage in cmps," in *ICPP*, 2009.
- [30] A. Naveh *et al.*, "Power and thermal management in the Intel Core Duo Processor," *Intel Technology Journal*, vol. 10, no. 2, 2006.
- [31] J. T. Pawlowski, "Hybrid memory cube: Breakthrough DRAM performance with a fundamentally re-architected DRAM subsystem," in *HOTCHIPS-23*, 2011.
- [32] M. Powell *et al.*, "Gated-Vdd: A circuit technique to reduce leakage in deep-submicron cache memories," in *ISLPED*, 2000.
- [33] M. Powell *et al.*, "Reducing leakage in a high-performance deep-submicron instruction cache," *IEEE Transactions on VLSI*, vol. 9, pp. 77-89, 2001.
- [34] A. L. Shimpi, "AMD's Steamroller detailed: 3rd generation Bulldozer core," 2012. Available: <http://www.anandtech.com/show/6201/amd-details-its-3rd-gen-steamroller-architecture>
- [35] A. Snaveley and D. M. Tullsen, "Symbiotic jobscheduling for a simultaneous multithreaded processor," in *ASPLOS-9*, 2000.
- [36] Standard Performance Evaluation Corporation, "SPEC CPU2006," <http://www.spec.org/cpu2006>.
- [37] A. Udipi *et al.*, "Rethinking DRAM design and organization for energy-constrained multi-cores," in *ISCA-37*, 2010.
- [38] S.-H. Yang *et al.*, "An integrated circuit/architecture approach to reducing leakage in deep-submicron high-performance I-caches," in *HPCA-7*, 2001.
- [39] S.-H. Yang *et al.*, "Exploiting choice in resizable cache design to optimize deep-submicron processor energy-delay," in *HPCA-8*, 2002.
- [40] C. Zhang *et al.*, "A highly configurable cache architecture for embedded system," in *ISCA-30*, 2003.
- [41] H. Zhou *et al.*, "Adaptive mode control: A static-power-efficient cache design," in *PACT-10*, 2001.